

Self-Consistent Model of Light-Induced Molecular Motion Around Metallic Nanostructures

Mathieu L. Juan,^{†,§} Jérôme Plain,^{*,†} Renaud Bachelot,[†] Pascal Royer,[†] Stephen K. Gray,^{*,‡} and Gary P. Wiederrecht[‡]

[†]Laboratoire de Nanotechnologie et d'Instrumentation Optique, ICD, Université de Technologie de Troyes, BP 2060 Troyes, France, and [‡]Center for Nanoscale Materials, Argonne National Laboratory, Argonne, Illinois 60439

ABSTRACT Azobenzene derivatives containing polymers deform when exposed to light with a wavelength in the principle absorption band associated with trans–cis isomerization of the azobenzene derivative molecule. When such polymers cover a metallic nanoparticle exposed to light near its surface plasmon resonance, which also happens to overlap with the azobenzene derivative absorption band, the resulting surface deformations are a novel measure or probe of the plasmonic near-field intensities. We developed a self-consistent model of the process by combining a Monte Carlo based model for the absorption and subsequent light-induced mass transport of the polymer with finite difference time domain computations of the electromagnetic fields around the nanoparticle that induce the absorption. The resulting self-consistent approach is shown to describe the key features of experimental observations concerning silver disk nanoparticles.

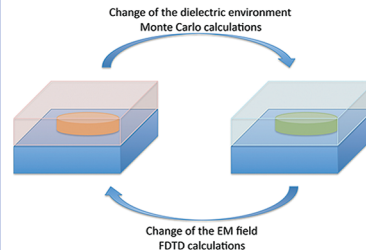
SECTION Nanoparticles and Nanostructures

The field of nanophotonics has attracted considerable attention due to unique optical physics at the nanoscale and the resulting potential applications of miniaturized structures. An important direction for nanophotonics is the fabrication of hybrid active nanostructures formed by coupling molecules to optical devices such as photonic crystals, plasmonic crystals, or integrated optical switches. A challenge for these studies is the ability to model the behavior of the active medium in the vicinity of a resonant photonic nanostructure by taking into account the parameters subject to dynamical evolution, such as chemical affinity, diffusion of molecules, and refractive index changes. Such a model will provide further opportunities in important nanophotonics applications of hybrid materials, such as sensing, SERS, nanophotolithography, and biolabeling. We tested such a model on a system which produces strong structural evolution under light irradiation.

The modeling of electromagnetic fields produced by plasmonic structures is a very active field of research, driven by wholly new optical phenomena and applications in diverse areas that include plasmonic metamaterials, integrated photonics, and field-enhanced sensors. Many key opportunities in plasmonics further require that the metal structure be surrounded by a dynamically changing dielectric material, particularly for studies of chemical affinity, plasmon-assisted photochemistry, near-field data storage, and light-assisted molecular diffusion.^{1,2} These studies are severely hampered, however, by the lack of a model that can simultaneously incorporate the evolution of both the electromagnetic field of the plasmonic structure and the evolution of the environmental topographic and dielectric spatial features during the given photoinduced process. A model that is self-consistent for both electromagnetic and structural changes in the hybrid material would be enormously

helpful in understanding and ultimately manipulating these two entities at the nanoscale. We report here a self-consistent model that successfully predicts the experimentally determined electromagnetic and structural changes of a photoresponsive plasmon-based hybrid nanomaterial. This is achieved through the development of a Monte Carlo (MC) based model for the absorption and subsequent light-induced mass transport of a photoresponsive polymer, combined with finite difference time domain (FDTD) computations that predict the changes in the electromagnetic fields around the plasmonic nanoparticle that induces the absorption.

The photoresponsive polymer is an azobenzene-based material that has been the focus of much interest for various applications.^{3,4} The surface topology of these polymers can distort in the presence of light with a wavelength in the principle absorption band associated with trans–cis isomerization of the azobenzene molecule. This remarkable phenomenon, which is also polarization-dependent, has been used to generate surface relief gratings^{5,6} and is relevant to optical information storage and processing. Recently, it has been used as a novel way of imaging confined electromagnetic fields since certain deformations can be associated with regions of high or low electric field intensity.^{7–10} For example, ref 7 considered silver disk-shaped nanoparticles coated with the polymer poly(methyl methacrylate) (PMMA) functionalized with azobenzene derivative Disperse Red 1 [DR1: 2-(ethyl(4-((4-nitrophenyl)azo)phenyl)amino)-ethanol] chromophores.⁷ As reported, after illumination with



Received Date: June 3, 2010

Accepted Date: June 30, 2010

Published on Web Date: July 07, 2010

532 nm light, the resulting polymer topology, measured by atomic force microscopy (AFM), is a partial reflection of the evanescent surface plasmon fields. These latter fields were determined via rigorous computational electrodynamics calculations on the initial, undistorted structure.⁷ In particular, certain regions corresponding to high near-field intensity can be correlated with holes or craters in the topography.

While Hubert et al.⁷ present compelling evidence for the correlation of the resulting surface topography with the near-field intensity inferred from calculations based on the fixed original structure, there are some noticeable differences. In particular, the actual light-induced spatial features near the nanoparticles are more removed and significantly wider than what would be expected on the basis of simply the electromagnetic field intensity. It is clear that a more complex process is occurring. Recently, we showed¹¹ that a relatively simple MC based model (photoinduced molecular diffusion model or PIMD model) involving translational motions of the azodye molecules could adequately reproduce the main features of the mass transport induced by a static electromagnetic field, including the polarization dependence. However, we will see below that this is just one component of correctly modeling the evolution of the topography involving high near-field intensities associated with plasmon resonance. In particular, we will show that the electromagnetic field itself must be allowed to adapt to the changing surface topography, and in turn, the topography must adjust to the changing electromagnetic field. As is well-known, resonant plasmonic nanostructures are very sensitive to the refractive index changes, thus allowing the development of plasmon-based sensors.^{2,12} As shown recently,¹⁰ the dynamics of the topography's changes is strongly correlated with dynamics of the local electromagnetic field driven by the plasmon resonance. However, ref 10 did not account for how the electromagnetic field itself can be modified by the evolving topographic changes. In order to take into account the local field changes during the irradiation process, a self-consistent model is proposed. Note that this new model could be easily updated to simulate resonance plasmon changes when metal nanoparticles interact with molecules in more complex systems. Our approach can be generalized to other resonant structures sensitive to the local dynamical environment changes, such as refractive-index-sensitive photonic crystals or plasmonic antennas surrounded by electrically driven liquid crystals.¹³

In this Letter, we develop a self-consistent model of the light-induced mass transport that couples the PIMD model of light-induced mass transport with rigorous electrodynamics information generated with the FDTD method, as schematically represented Figure 1a. We apply this PIMD-FDTD approach to the computation of the surface topography around disk-shaped silver nanoparticles and demonstrate how relatively deep craters can form near the nanoparticles. These results are in very good agreement with experimental observations and point to the importance of a self-consistent approach involving both field topography and field topographic response due to the electromagnetic field and electromagnetic field response due to the topography.

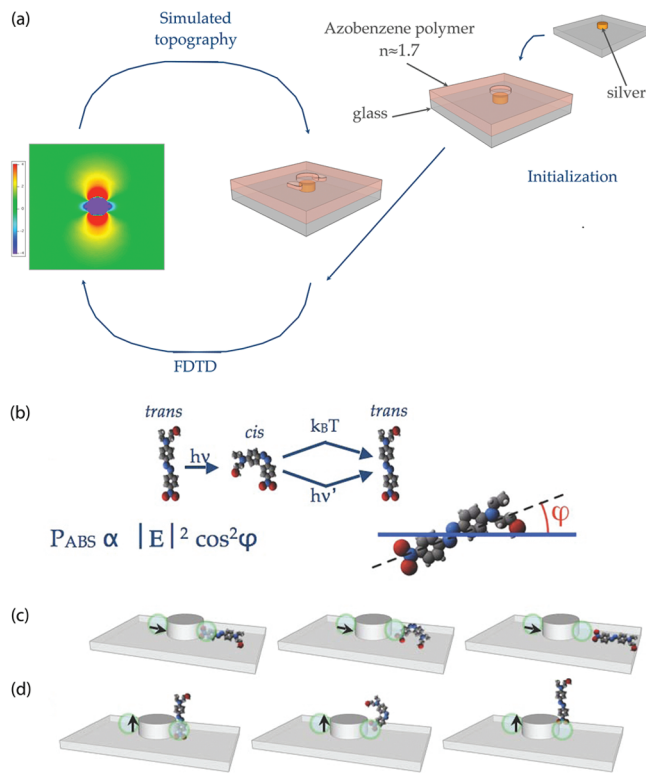


Figure 1. (a) Schematic representation of the coupled Monte Carlo-FDTD approach. Features and consequences of the PIMD model of ref 11. (b) Each molecule undergoes a trans-cis-trans isomerization cycle upon absorption of a photon, leading to a worm-like motion along the molecule's electronic dipole axis. (c) Molecular motion induced along a near-field component that is parallel to the film, leading to the depletion of molecules from regions of high intensity. (d) Molecular motion along a near-field component that is normal to the film and nanoparticle top, leading to a raised topography.

We first briefly outline the main components of the PIMD model¹¹ as it applies to a fixed electromagnetic field distribution, E . We should note that there are alternative theoretical models based on quite different physical assumptions.^{14–18} However, each of these models cannot explain all aspects of the phenomenon (polarization dependencies, photoinduced molecular orientation, orientational hole burning).^{3,11} In our PIMD model, we begin with a system of randomly oriented azobenzene-like molecules within the region of space corresponding to the polymer material. Physical space is divided up into many small cubes, and each cube corresponding to the polymer will initially contain, on average, a number density consistent with the case to be studied. Each molecule must absorb a photon to undergo an isomerization, and the PIMD method is used to implement that on average this absorption probability is given by $P_{\text{abs}} \propto |E|^2 \cos^2 \varphi$, where φ is the angle between the direction of the local incident field E and the molecular dipole (see Figure 1a). The movement of the molecule is assumed to occur along the axis of the molecular dipole, as described by the worm-like translational model proposed by Lefin et al.¹⁷ The molecules thus move in and out of these cubes, and the overall polymer is assumed to be the union of these cubes since the molecules are functionalized to the polymer and thus push or pull it along.

Near the original surface of the polymer, molecules are allowed to move up into the air, leading to polymer surface elevation; they are also allowed to move down into the bulk of the polymer, leading to polymer surface lowering. These ideas alone are sufficient to guarantee the experimentally observed polarization effects and the fact that material will tend to move from regions of higher to lower electromagnetic field intensity.¹¹ The latter effect is somewhat akin to the previously proposed idea of motion due to a gradient force based on $|E|^2$, but it is important to realize that our result is not directly related to actual optical forces, which are likely too weak to generate mass transport. Figure 1 indicates some features and further consequences of the model. In particular we should note that a crater is not necessarily the only outcome of a high near-field spot. As indicated in Figure 1c,d, depending on the near-field polarization, it is also possible to obtain an elevation. These subtle but logical features are discussed in more detail in ref 9. In order to refine our PIMD model and allow it to be used to study different systems, several other key elements are added.

(i) To account for the mechanical aspect of the photoinduced migration, a dye molecule moves from a hole in the polymer matrix to another hole. A hole is an area with free space available in the polymer matrix. This aspect accounts for the free space consideration inherent to the mechanical migration.

(ii) Related to the matrix aspect of the polymer, the motion of dye molecule induces close-range perturbations through local interactions (e.g., van der Waals interactions).

(iii) In parallel to short-range interactions, long-range interactions are induced by the polymer chain. Due to the dye molecules being grafted to the polymer, each time a molecule moves, perturbations are applied at the positions and orientations of a set of n molecules grafted to the same chain. These molecules are selected by accounting for the grafting density, the molecular weight, and the radius of gyration of the polymer. In our PIMD model, the path of thermal relaxation is not directly considered but is indirectly taken into account in the random reorientations.

The PIMD model above involves, for a fixed electromagnetic field $E(x,y,z)$, several thousand iterations (i.e., passes through all of the molecules in the polymer portion of the system) and slight movements of these molecules according to the above rules until a stationary state has been achieved.¹¹

Our new, self-consistent model is as follows. For a given initial system topography, we carry out rigorous FDTD calculations for a plasmonic nanostructure sitting on glass with a coating of PMMA-DR1 (refraction index = 1.72 is kept constant in each occupied box). In these calculations, a monochromatic incident field consistent with the experimental setup (CW, $\lambda = 532$ nm linearly polarized) is used, and the propagation time is taken to be sufficiently long (typically 200 fs) such that a steady-state field distribution has been achieved. We actually sample the last optical cycle of this FDTD calculation, taking a time sequence $E(t_1), E(t_2), \dots, E(t_{20})$ of the electromagnetic field. One can then refine the PIMD model by accounting for the time dynamics of the photoisomerization process; a dye molecule undergoing photoinduced migration cannot reabsorb another photon for a given time. Thus, a molecule absorbing a photon at t_i in the electric field $E(t_i)$ could reabsorb a photon at $E(t_i + \tau)$. A scaling law is applied to the

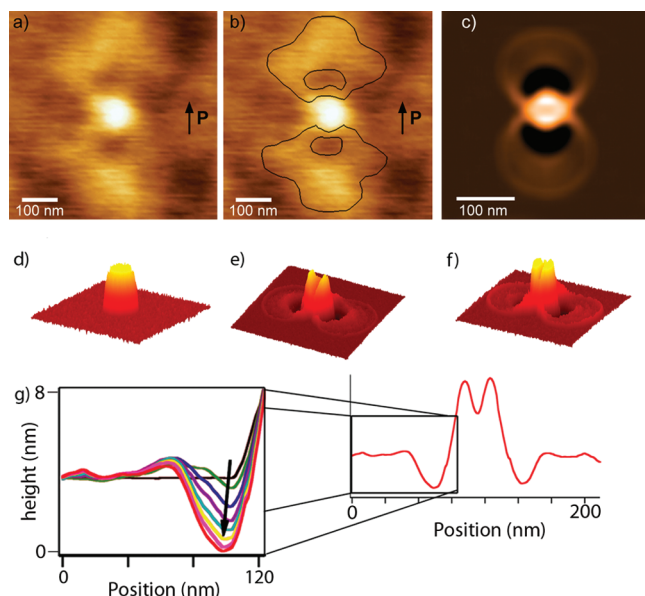


Figure 2. The evolution of the PMMA-DR1 surface topography around a silver disk nanoparticle under 532 nm illumination. (a,b) Experimental results obtained with a 20 min exposure at $\lambda = 532$ nm with a power of 90mW/cm^2 . (b) Same image as (a), but we have overlaid lines to highlight the major topological changes. (c) Calculated topography obtained after eight macrocycles. 3D representations of the calculated topography after (d) zero macrocycle calculations (Initial configuration), (e) three macrocycles, and (f) eight macrocycles. (g) Topography profile along the polarization axis after eight macrocycles. Enlarged is the variation of the topography profile along the polarization as a function of the macrocycle number, from zero to eight.

typical trans-cis-trans isomerization time τ , several orders of magnitude longer than an optical cycle, to allow the numerical implementation. After a given number of such PIMD iterations, large enough to obtain sensible topographic modifications, a new FDTD calculation is performed with the current topography, and the entire process is repeated. The FDTD calculation followed by the PIMD iterations to resolve the transitory topography is referred to as a macrocycle. On the order of 8–10 such macrocycles are generally required to achieve a steady-state topography. The calculations stop at the macro-scale equilibrium (i.e., when the topography does not change). Considering the microscopic equilibrium (i.e., at the molecular scale), the molecules are not necessarily at the equilibrium. For realistic, three-dimensional problems involving metallic nanostructures, it should be noted that this PIMD–FDTD procedure can require substantial computing resources. The calculations described below were carried out with a parallel implementation of the procedure and run for several hours on 64 processors of a Beowulf cluster.

We applied the above self-consistent PIMD–FDTD procedure to the evolution of the topography around a silver disk nanoparticle of diameter 50 nm and height 50 nm sitting on glass with a coating of PMMA-DR1. For comparison, experimental measurements have been performed in parallel. We used a 532 nm CW doubled Nd:YAG laser with an intensity of 90mW/cm^2 . Both experimental and calculation results are presented in Figure 2.

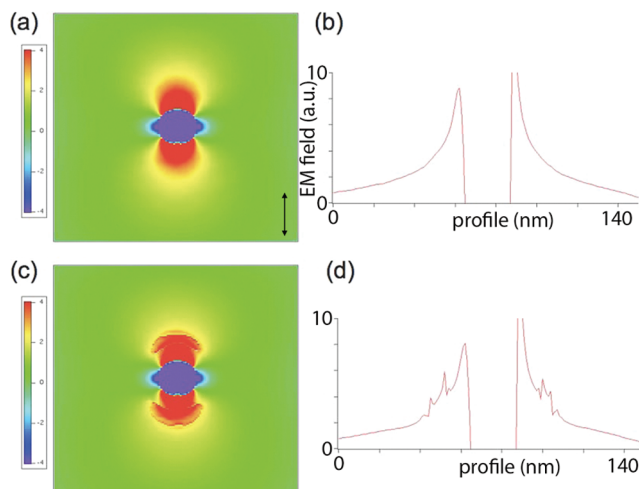


Figure 3. The y component of the electric field associated with the stages of evolution of the self-consistent procedure. The initial E_y component is given in (a) and (b), and the final E_y component, after eight macrocycles of the PIMD-FDTD procedure, is given in (c) and (d). The right-hand images correspond to $x-y$ profiles with $z = 48$ nm inside of the 60 nm height PMMA-DR1 layer. The left-hand cuts are along y , the polarization direction.

Note that the features obtained along the polarization axis and presented in Figure 2b,c are in good agreement, except on the top of the particle where there is a slight difference. Figure 2d represents the initial system configuration corresponding to a silver disk of diameter 50 nm and height 50 nm sitting on glass with a coating of PMMA-DR1. The resulting topography after three macrocycles is depicted in Figure 2e. Small craters are evident near the nanoparticle edges along the direction of the incident polarization. The final, converged result after eight macrocycles, Figure 2f, shows that the craters have grown in size. These results are in good accord with the experimental observations (Figure 2a,b) and clearly show the importance of adapting a self-consistent approach to determining the photoinduced mass transport. Figure 2g represents the evolution of the calculated profile as a function of the number of macrocycles. There is a clear enhancement of the depth and a broadening of the hole close to the structure. Furthermore, after eight macrocycles, a bump extending about 80 nm from the central dip is evident that is in very good agreement with the experimental findings. From a comparison between the response calculated with the simple PIMD model (shown in Figure 2g in green) and the response obtained after eight cycles (shown in Figure 2g in red), we conclude that a complete quantitative description of the system could be uniquely obtained after eight macrocycles. The numerical effort relative to just one FDTD calculation on the fixed structure⁷ is significantly more demanding, and of course, it is also more demanding than our previous model involving structural changes but keeping the electric field fixed.¹¹ Full simulations can require up to 24 h on 64 processors of a parallel computer. Nonetheless, we believe that the physical information regarding the mechanistic details justifies such effort.

The electromagnetic fields, of course, also evolve during the self-consistent process that leads to the final topographic structure in Figure 2. The y component of E , E_{y*} , is along the incident polarization axis and generally exhibits the largest

near-field enhancements. Figure 3a,b depicts the initially computed E_y values. The cross cut through the polarization direction, Figure 3b, shows in particular the relatively sharp near-field enhancements close to the particle edges. The final E_y component (after eight macrocycles of the PIMD-FDTD procedure) is broader and choppier as shown in Figure 3c,d.

In conclusion, we presented a self-consistent PIMD-FDTD procedure for understanding photoinduced mass transport in metallic nanostructures. The procedure was applied to the problem of silver disk nanoparticles coated with PMMA-DR1, a polymer containing an azobenzene derivative. The resulting surface topographies showed large craters near the nanoparticles oriented along the incident polarization direction, in very good agreement with experimental observations. Such self-consistent modeling, while more computationally intensive than simply the PIMD model applied to a fixed electromagnetic field, is expected to be essential in interpreting and predicting the results of experiments on dynamical media interacting with other complex resonant optical systems (photonic crystals, plasmonic crystals, optical sensors, ...).

AUTHOR INFORMATION

Corresponding Author:

*To whom correspondence should be addressed. jerome.plain@utt.fr (J.P); gray@anl.gov (S.K.G.).

Present Addresses:

[§] ICFO, Spain.

ACKNOWLEDGMENT The authors are grateful to C. Hubert for helpful discussions. One of the author Ph.D. research (M.J.) is supported by the European Social Fund and the Conseil Général de l'Aube (district grant). This work was financially supported by the ANR (Programme blanc Photohybrid 2007). Use of the Center for Nanoscale Materials and work at Argonne National Laboratory were supported by the U.S. Department of Energy, Office of Science, Office of Basic Energy Science, under Contract No. DE-AC02-06CH11357.

REFERENCES

- 1) Jain, P. K.; Huang, X.; El-Sayed, I. H.; El-Sayed, M. A. Review of Some Interesting Surface Plasmon Resonance-Enhanced Properties of Noble Metal Nanoparticles and Their Applications to Biosystems. *Plasmonics* **2007**, 2, 107–118.
- 2) Anker, J. N.; Hall, W. P.; Lyandres, O.; Shah, N. C.; Zhao, J.; Van Duyne, R. P. Biosensing with Plasmonic Nanosensors. *Nat. Mater.* **2008**, 7, 442–453.
- 3) Natansohn, A.; Rochon, P. Photoinduced Motions in Azo-Containing Polymers. *Chem. Rev.* **2002**, 102, 4139–4175.
- 4) Cojocariu, C.; Rochon, P. Light-Induced Motions in Azobenzene-Containing Polymers. *Pure Appl. Chem.* **2004**, 76, 1479–1497.
- 5) Rochon, P.; Batalla, E.; Natansohn, A. Optically Induced Surface Gratings on Azoaromatic Polymer Films. *Appl. Phys. Lett.* **1995**, 66, 136–138.
- 6) Kim, D. Y.; Tripathy, S. K.; Li, L.; Kumar, J. Laser-Induced Holographic Surface Relief Gratings on Nonlinear Optical Polymer Films. *Appl. Phys. Lett.* **1995**, 66, 1166–1168.
- 7) Hubert, C.; Rumyantseva, A.; Lerondel, G.; Grand, J.; Kotscheev, S.; Billot, L.; Vial, A.; Bachelot, R.; Royer, P.; Chang,

S.; et al. Near-Field Photochemical Imaging of Noble Metal Nanostructures. *Nano Lett.* **2005**, *5*, 615–619.

(8) Gilbert, Y.; Bachelot, R.; Royer, P.; Bouhelier, A.; Wiederrecht, G.; Novotny, L. Longitudinal Anisotropy of the Photoinduced Molecular Migration in Azobenzene Polymer Films. *Opt. Lett.* **2006**, *31*, 613–615.

(9) Hubert, C.; Bachelot, R.; Plain, J.; Kotscheev, S.; Lerondel, G.; Juan, M.; Royer, P.; Zou, S.; Schatz, G. S.; Wiederrecht, G.; et al. Near-Field Polarization Effects in Molecular Motion Induced Photochemical Imaging. *J. Phys. Chem. C* **2008**, *112*, 4111–4116.

(10) Juan, M. L.; Plain, J.; Bachelot, R.; Vial, A.; Royer, P.; Gray, S. K.; Montgomery, J. M.; Wiederrecht, G. P. Plasmonic Electromagnetic Hot Spots Temporally Addressed by Photoinduced Molecular Displacement. *J. Phys. Chem. A* **2009**, *113*, 4647–4651.

(11) Juan, M. L.; Plain, J.; Bachelot, R.; Royer, P.; Gray, S. K.; Wiederrecht, G. P. Multiscale Model for Photoinduced Molecular Motion in Azo Polymers. *ACS Nano* **2009**, *3*, 1573–1579.

(12) Barbillon, G.; Bijeon, J.-L.; Plain, J.; de la Chapelle, M. L.; Adam, P.-M.; Royer, P. Biological and Chemical Gold Nano-sensors Based on Localized Surface Plasmon Résonance. *Gold Bulletin* **2007**, *40*, 240–244.

(13) Berthelot, J.; Bouhelier, A.; Huang, C.; Margueritat, J.; des Francs, G. C.; Finot, E.; Weeber, J.-C.; Dereux, A.; Kostcheev, S.; Ahrach, H. I. E.; et al. Tuning of an Optical Dimer Nanoantenna by Electrically Controlling Its Load Impedance. *Nano Lett.* **2009**, *9*, 3914–3921.

(14) Barrett, C.; Natansohn, A. L.; Rochon, P. L. Mechanism of Optically Incribed High-Efficiency Diffraction Gratings in Azo Polymer Films. *J. Phys. Chem.* **1996**, *100*, 8836–8842.

(15) Pedersen, T. G.; Johansen, P. M. Mean-Field Theory of Photo-induced Molecular Reorientation in Azobenzene Liquid Crystalline Side-Chain Polymers. *Phys. Rev. Lett.* **1997**, *79*, 2470–2473.

(16) Barada, D.; Fukuda, T.; Itoh, M.; Yatagai, T. Numerical Analysis of Photoinduced Surface Relief Grating Formation by Particle Method. *Opt. Rev.* **2005**, *12*, 271–273.

(17) Lefin, P.; Fiorini, C.; Nunzi, J. Anisotropy of the Photo-Induced Translation Diffusion of Azobenzene Dyes in Polymer Matrices. *Pure Appl. Opt.* **1998**, *7*, 71–82.

(18) Bellini, B.; Ackermann, J.; Klein, H.; Graves, C.; Dumas, P.; Safarov, V. Light-Induced Molecular Motion of Azobenzene-Containing Molecules: A Random-Walk Model. *J. Phys.: Condens. Matter* **2006**, *18*, S1817–S1835.